

# Query2GMM: Learning Representation with Gaussian Mixture Model for Reasoning over Knowledge Graphs

Yuhan Wu\*

East China Normal University

Yuanyuan Xu\*<sup>†</sup>

Zhejiang Lab, University of New South Wales

Wenjie Zhang

University of New South Wales

Ying Zhang

University of New South Wales

## Abstract

Logical query answering over Knowledge Graphs (KGs) is a fundamental yet complex task. A promising approach to achieve this is to embed queries and entities jointly into the same embedding space. Research along this line suggests that using multi-modal distribution to represent answer entities is more suitable than uni-modal distribution, as a single query may contain multiple disjoint answer subsets due to the compositional nature of multi-hop queries and the varying latent semantics of relations. However, existing methods based on multi-modal distribution roughly represent each subset without capturing its accurate cardinality, or even degenerate into uni-modal distribution learning during the reasoning process due to the lack of an effective similarity measure. To better model queries with diversified answers, we propose Query2GMM for answering logical queries over knowledge graphs. In Query2GMM, we present the GMM embedding to represent each query using a univariate Gaussian Mixture Model (GMM). Each subset of a query is encoded by its cardinality, semantic center and dispersion degree, allowing for precise representation of multiple subsets. Then we design specific neural networks for each operator to handle the inherent complexity that comes with multi-modal distribution while alleviating the cascading errors. Last, we define a new similarity measure to assess the relationships between an entity and a query's multi-answer subsets, enabling effective multi-modal distribution learning for reasoning. Comprehensive experimental results show that Query2GMM outperforms the best competitor by an absolute average of 5.5%. The source code is available at <https://anonymous.4open.science/r/Query2GMM-C42F>.

## 1 Introduction

Knowledge Graphs (KGs) are structured heterogeneous graphs, which are constructed based on entity-relation-entity triplets. A fundamental task in knowledge graph reasoning, known as *logical query answering*, involves answering First-Order Logic (FOL) queries over KGs using operators including existential quantification ( $\exists$ ), conjunction ( $\wedge$ ), disjunction ( $\vee$ ) and negation ( $\neg$ ). This has wide real-life applications, such as web search [1, 2] and medical research [3, 4], among which real-life KGs often exhibit incompleteness according to the Open World Assumption [5]. To handle such incompleteness, numerous efforts have been devoted to developing neural models for complex logical query answering [6, 7, 8, 9, 10, 11, 12, 13, 14, 15, 16, 17].

\*Yuhan Wu and Yuanyuan Xu are the joint first authors.

<sup>†</sup>Yuanyuan Xu is the corresponding author.

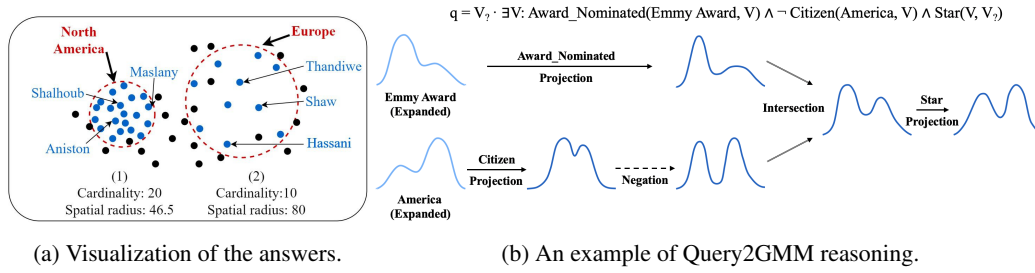


Figure 1: (a) Visualization of the answer distribution of the query "Who has been nominated for Emmy Award?" (b) Illustration of reasoning of Query2GMM on the query "What are the movies starring non-American actors who have been nominated for Emmy Award?" (2-modal distribution).

Along this line, most existing approaches for logical reasoning over KGs work under the assumption that answer entities of each query typically follow a uni-modal distribution [4, 11, 18, 12, 8]. Based on this assumption, they design various embedding backbones based on geometric structures [18, 12, 8], probabilistic distributions [11, 4, 9] and other basis [13, 14, 19, 20]. These structures are used to embed logical queries and answer entities in the same embedding space, where all answer entities of a query are expected to be encompassed within a large single region. For example, Q2B [18] develops the box embedding for each query and the point embedding for each entity, assuming that all answer entities for a query are inside or close to the box region corresponding to that query. PERM [4] applies a multivariate Gaussian distribution to encode the semantic location and spatial query area for each query's answers with a smooth boundary, following the same assumption. However, this broad assumption compromises the expressiveness of logical queries and entities, as it inevitably includes many false positives in the large single region for a query.

Recently, research has found that the ideal query embedding may follow a multi-modal distribution<sup>3</sup> in the embedding space due to the compositional nature of multi-hop queries [6]; additionally, a relation can have multiple unknown latent semantics for different concrete triples [21]. For instance, given a logical query "Who has been nominated for Emmy Award?", the relation "Award Nominated" has several latent semantics including Actor Award, Artist Award, Actress Award, etc. Consequently, the intermediate entity set for individuals nominated for the Emmy Award may vary in terms of gender, nationality and other factors, leading to answer entities forming multiple disjoint subsets, as shown in Fig. 1a. A few recent studies aim to model the diversity of answer entities by designing appropriate embedding backbones that encode multiple disjoint subsets of answer entities. Specifically, NMP-QEM [10] leverages multivariate Gaussian mixture distribution to encode multiple disjoint answer subsets of each query, but it must transform the Gaussian mixture distribution into a single centroid vector when measuring relationships between entities and queries in the embedding space. As a result, NMP-QEM degenerates to uni-modal distribution learning during the reasoning process. Query2Particles [6] proposes to encode each query with a set of vectors (particles), where each vector represents an answer subset according to its setting. However, this is problematic that it neglects the cardinality of these subsets, leading to an ambiguous answer entity set and compromising the performance of query answering.

Despite the potential advantages of multi-modal distribution modelling, existing methods struggle to learn accurate subset representation and even fail to assess the relationships between entities and queries in the multi-modal distribution context, limiting and violating the expressiveness of the query embedding. To further improve embedding quality, several challenges need to be addressed:

**Challenge I: How to accurately quantify different answer subsets of each query?** In practice, answer entities to each query may contain multiple disjoint subsets. Different from the uni-modal distribution, it is essential to accurately characterize the semantic center and cardinality of each subset in the multi-modal distribution context, which can provide prompts for reasoning and answer retrieval. Existing methods [6, 10] either neglect the cardinality or regard spatial query area as the cardinality. In fact, we observe from Fig. 1a that a relatively small area (left) contains more answer entities than the large one (right), which is contradicted by the radius of the spatial query area. This

<sup>3</sup>A multi-modal distribution has two or more distinct peaks in its probability density function.

leads to sub-optimal query embedding and compromises logical reasoning. Thus, it is necessary to accurately quantify each subset for high-quality query embedding.

**Challenge II: How to judiciously leverage the advantage of Gaussian distribution?** Multivariate Gaussian distribution has been applied in logical query embedding [4, 10], showing the effectiveness of the expressive parameterization of decision boundaries. Despite some attempts, it is intractable to effectively employ Gaussian distribution for the query embedding with multi-modal distribution due to the following reasons: (1) It typically involves the computation of the covariance matrix (e.g., inverse operation) for the multivariate Gaussian distribution, incurring expensive computational costs. (2) There is no feasible solution to measure the relationships between an entity and multiple-answer subsets of a query based on the Gaussian mixture distribution. NMP-QEM [10] transfers multivariate Gaussian mixture distribution into a single centroid center vector with weighted sum operation and then uses  $L_1$  distance to compute the similarity between an entity and a query, which is fundamentally uni-modal distribution modelling for logical reasoning. Hence, it is challenging to effectively employ the Gaussian distribution for modelling multiple disjoint answer subsets.

In this paper, we study the problem of modelling the diversity of answers for logical reasoning over knowledge graphs by addressing the above challenges. We propose Query2GMM, a novel query embedding approach for complex logical query answering. Concretely, we present the GMM embedding to represent each query based on a univariate Gaussian mixture model. Each subset of a query is encoded by its cardinality, semantic center and dispersion degree, elegantly corresponding to the normalized probability, mean value and standard deviation of a univariate Gaussian mixture model. This can offer a more appropriate and precise representation of each subset (**Challenge I**). Additionally, Query2GMM can independently learn these three parameters by using the Cartesian product of a  $d$ -dimensional univariate Gaussian mixture distribution as the representation of the answer set, which enables Query2GMM fitting complex answer sets as well as maintaining the linear complexity of the model. Last, we define a new similarity measure (called mixed Wasserstein distance) based on the Wasserstein distance [22] and the upper bound of Kullback-Leibler (KL) divergence, allowing for computing the relationships between entities and multiple answer subsets. The mixed Wasserstein distance forms the foundation of the multi-modal distribution modelling during the reasoning process (**Challenge II**). Extensive experimental results demonstrate that our Query2GMM achieve an average absolute improvement of 5.5% compared to the best baseline.

## 2 Preliminaries

**Knowledge Graphs.** A knowledge graph is denoted as  $\mathcal{G} = \{V, R, \Theta\}$ , where  $V$ ,  $R$  and  $\Theta$  refer to the entity set, relation set and fact triplet set, respectively. To record the basic connections of the knowledge graph, a binary relational function:  $\mathcal{V} \times \mathcal{V} \rightarrow \{1, 0\}$  is used to memory triplets joined by each  $r_j \in R$  with head entity  $h_i \in V$  and tail entity  $\theta_k \in V$ , where  $r_j(h_i, \theta_k) = 1$  if and only if  $(h_i, r_j, \theta_k)$  is a factual triple.

**First-Order Logic (FOL).** FOL queries in the literature involve logical operations including existential quantification ( $\exists$ ), conjunction ( $\wedge$ ), disjunction ( $\vee$ ) and negation ( $\neg$ ). We use FOL queries in its Disjunctive Normal Form (DNF) [18], which represents FOL queries as a disjunction of conjunctions for effective computation.

**Computation Graphs.** Following the convention, a logical query is represented by a Directed Acyclic computation Graph (DAG):  $\mathcal{Q} = \{U, R, L\}$ , where  $U = \{\tilde{U}, U_\gamma\}$  denotes the node set with  $\tilde{U}$  referring to the anchor nodes that are the source nodes of DAG and  $U_\gamma$  denoting the variable nodes,  $R$  denotes the relation set that is the same as the relation set of  $\mathcal{G}$ , and  $L$  denotes logical operations. Fig. 1b gives an instantiated computation graph on the Query2GMM approach.

**Problem Statement.** In this paper, we aim to model the ideal distribution of answer entities of logical queries, i.e., multi-modal distribution, along the line of the query embedding approach. Concretely, queries and entities are mapped into the same low-dimensional embedding space, associating each logical operator for entity sets with a transformation in the embedding space. The aim of answering logical queries is to find a set of entities as answers such that these entities' embeddings should be included or close to the embedding of the given query in the embedding space.

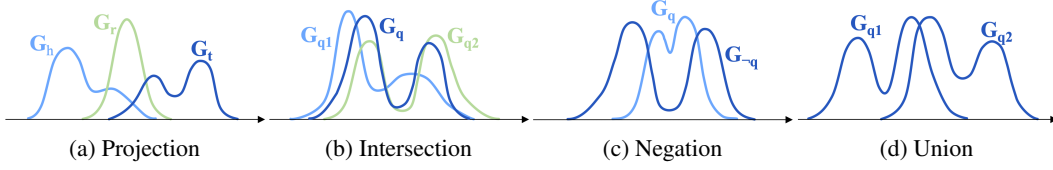


Figure 2: Visualization of logical operator transformation. The input embeddings are represented in light blue and green colors, while the output is shown in deep blue.

### 3 The proposed Query2GMM

#### 3.1 GMM embeddings for Entities and Queries

In Query2GMM, we design GMM embedding, i.e., univariate Gaussian mixture model for query embedding, to represent each query. This choice is motivated by the fact that mixed Gaussian distributions can approximate any random distribution arbitrarily well [23]. The cardinality, semantic center, and dispersion degree of each subset of the answer entity set for a query can be intuitively and elegantly represented by the normalized probability, mean value, and standard deviation of a univariate Gaussian mixture distribution, respectively. To better fit complex and diversified answers, we expect that each dimension can be independently learned to explore different information, thus we leverage the Cartesian product for the representation of each sub-distribution<sup>4</sup>. Formally, GMM embedding for a query  $q$  is represented as  $\mathbf{G}_q = [\mathbf{g}_1, \mathbf{g}_2, \dots, \mathbf{g}_k] \in \mathbb{R}^{k \times 3d}$ , where  $k$  is the number of components in the Gaussian mixture distribution. The embedding of each subset with  $d$ -ary Cartesian product of three semantic components can be defined as

$$P(x|\theta) = \sum_{i=1}^k \alpha_i \Phi(x|\mu_i, \sigma_i), \quad \sum_{i=1}^k \alpha_i^j = 1, \quad \text{for } j = 1, 2, \dots, d, \quad (1)$$

$$\mathbf{g}_i = \mathbf{g}_i^1 \times \mathbf{g}_i^2 \times \dots \times \mathbf{g}_i^d = [(\alpha_i^1, \mu_i^1, \sigma_i^1), \dots, (\alpha_i^d, \mu_i^d, \sigma_i^d)]. \quad (2)$$

Equivalently, Eq. (2) can be formulated as  $\mathbf{g}_i = [\alpha_i; \mu_i; \sigma_i]$ ,  $i = 1, 2, \dots, k$ . Here,  $\alpha_i \in \mathbb{R}^d$  refers to the normalized cardinality proportion of a subset,  $\mu_i \in \mathbb{R}^d$  determines the semantic center of a subset and  $\sigma_i \in \mathbb{R}^d$  represents the dispersion degree of answers in a subset. For the complex query answering on large-scale knowledge graphs, there are often one-to-many relationships between entities and queries. Different from existing works that only consider the semantic center for an entity, in this paper, each entity of KGs is represented by a univariate Gaussian distribution embedding with learnable mean value and standard deviation (called Gaussian embedding), i.e.,  $\mathbf{G}_e = [\mu_e; \sigma_e] \in \mathbb{R}^{2d}$ ,  $\mu_e \in \mathbb{R}^d$ ,  $\sigma_e \in \mathbb{R}^d$ . Here standard deviation serves as the scaling of the distribution, enabling entity embeddings to approach multiple query embeddings with different semantics simultaneously. We also use a univariate Gaussian distribution to represent the relation embedding, i.e.,  $\mathbf{G}_r = [\mu_r; \sigma_r] \in \mathbb{R}^{2d}$ ,  $\mu_r \in \mathbb{R}^d$ ,  $\sigma_r \in \mathbb{R}^d$ .

Last, for effective computation, we separately learn a trainable transformation matrix for the normalized probability, mean value, and standard deviation. This allows us to formulate the embedding representation of the entity set that corresponds to the provided anchor entity as follows:

$$\mathbf{G}_q = [\mathbf{T}_\alpha; \mathbf{T}_\mu; \mathbf{T}_\sigma], \quad \mathbf{T}_\alpha = \mathbf{O}_\alpha, \quad \mathbf{T}_\mu = \mu_e + \mathbf{O}_\mu, \quad \mathbf{T}_\sigma = \sigma_e + \mathbf{O}_\sigma, \quad (3)$$

where  $\mathbf{O}_\alpha \in \mathbb{R}^{k \times d}$ ,  $\mathbf{O}_\mu \in \mathbb{R}^{k \times d}$  and  $\mathbf{O}_\sigma \in \mathbb{R}^{k \times d}$  are the learnable expansion matrices for the normalized probability, mean value, and standard deviation, respectively. Next, we introduce specific neural models of FOL operations, including projection, intersection, negation and union.

#### 3.2 Projection

Given a GMM embedding  $\mathbf{G}_h \in \mathbb{R}^{k \times 3d}$  of the input head entity set and Gaussian embedding  $\mathbf{G}_r \in \mathbb{R}^{2d}$  of the input relation, the projection operator aims to obtain the tail entity set connected

<sup>4</sup>In our context, we use the terms 'subset' and 'sub-distribution' interchangeably.

with any entity in the head entity set with the given relation (see Fig. 2a). Unlike uni-modal distribution learning, it is challenging to learn the overall transformation from the input entity set to the target entity set for relation modelling in the multi-modal distribution context [6, 10]. To address it, we employ a distributed gate [24] to control the different adjustment directions and magnitudes of different subsets of the head entity set based on the input relation, which is formulated as

$$\mathbf{G}_{r_{aug}} = [\boldsymbol{\alpha}_{r_{aug}}; \mathbf{G}_r], \quad \mathbf{g}_t = \sigma(\text{LayerNorm}(\mathbf{W}_g \mathbf{G}_{r_{aug}} + \mathbf{U}_g \mathbf{G}_h)) \quad (4)$$

$$\tilde{\mathbf{G}}_h = \text{ReLU}(\text{LayerNorm}(\mathbf{W}_h \mathbf{G}_{r_{aug}}) + \mathbf{U}_h \mathbf{G}_h), \quad \tilde{\mathbf{G}}_t = \mathbf{g}_t \odot \mathbf{G}_h + (1 - \mathbf{g}_t) \odot \tilde{\mathbf{G}}_h \quad (5)$$

where  $\boldsymbol{\alpha}_{r_{aug}} \in \mathbb{R}^d$  is the learnable normalized probability vector to formally align the dimension of relation embedding with that of the entity set embedding.  $\sigma(\cdot)$  is the sigmoid function, and  $\mathbf{g}_t$  is the distributed gate to make different adjustments with  $k$  subsets with the same relation.  $\text{LayerNorm}(\cdot)$  is the layer normalization [25], and  $\mathbf{W}_g, \mathbf{U}_g, \mathbf{W}_h$  and  $\mathbf{U}_h$  are parameter matrices. By Eqs. (4) and (5), we get the one-to-one mapping relationship between the tail entity set and head entity set. Then we employ the self-attention network [26] to fine-tune the subsets of the generated final tail entity set based on current relative position, cardinality and dispersion degree:

$$\mathbf{G}_t = \text{Attention}(\tilde{\mathbf{G}}_t \mathbf{W}_Q, \tilde{\mathbf{G}}_t \mathbf{W}_K, \tilde{\mathbf{G}}_t \mathbf{W}_V), \quad \text{Attention}(\mathbf{Q}, \mathbf{K}, \mathbf{V}) = \psi\left(\frac{\mathbf{Q}\mathbf{K}^T}{\sqrt{3d}}\right)\mathbf{V}. \quad (6)$$

where  $\psi(\cdot)$  is the Softmax function. This approach allows the  $k$  sub-distributions to collaborate, enabling them to cover as many correct answers as possible according to their individual roles.

### 3.3 Intersection

With  $m$  GMM embeddings as the input, the intersection operator aims to get the GMM embedding of the target entity set that covers the  $m$ -intersected answer areas of the input sets (see Fig. 2b). Here  $m$ -intersected indicates that the output of the intersection operator should encompass all  $m$  sets of inputs, although they may have varying degrees of overlap (e.g., 2-intersected, 3-intersected). Previous works based on Gaussian distribution [4, 10] handle the  $m$ -intersection problem by sequentially executing a series of pairwise-intersections, which raises several issues below. (1) To obtain the  $m$ -intersected answer areas of all  $m$  input sets through pairwise intersection, there are  $\frac{m!}{2!}$  possible processing orders. Yet, these studies do not provide an optimal execution order or guarantee the permutation invariance of execution orders. (2) The  $m-1$  chain executions for the intersection leads to severe cascading errors [27], which negatively impacts the model’s performance.

To overcome the above drawbacks, we design a co-attention model to directly derive the  $m$ -intersected areas of  $m$  input entity sets. This model can concurrently allocate and aggregate crucial information from both the inter-query level and inter-subset level to fit the candidate entity set. Concretely, we first compute the overall similarity between  $m$  input GMM embeddings and then obtain the inter-query level result using cross attention network:

$$\mathbf{G}'_q = \sum_{i=1}^m \mathbf{a}_i \odot \mathbf{G}_{q_i}, \quad \mathbf{a}_i = \frac{\exp(\text{MLP}(\mathbf{G}_{q_i}))}{\sum_{j=1}^m \exp(\text{MLP}(\mathbf{G}_{q_j}))}. \quad (7)$$

By Eq. (7), the output embedding is constrained by existing composition paradigms of the input GMM embeddings. To better encapsulate the interaction among  $m * k$  subsets, we employ the self-attention network to capture inter-subset level intersections based on global attention and then utilize the attention pooling [28] to adaptively generate the inter-subset level result. The learning process can be formulated as

$$\tilde{\mathbf{G}} = \text{Attention}(\mathbf{G}\mathbf{W}_Q, \mathbf{G}\mathbf{W}_K, \mathbf{W}_V), \text{ where } \mathbf{G} = [\mathbf{G}_{q_1}; \mathbf{G}_{q_2}; \dots; \mathbf{G}_{q_m}] \in \mathbb{R}^{(m*k)*3d} \quad (8)$$

$$\text{PoolingAttention}_k(\tilde{\mathbf{G}}) = \text{AttentionBlock}(\mathbf{S}, rFF(\tilde{\mathbf{G}})), \quad (9)$$

$$\text{AttentionBlock}(\mathbf{X}, \mathbf{Y}) = \text{LayerNorm}(\mathbf{H} + rFF(\mathbf{H})), \quad (10)$$

$$\mathbf{H} = \text{LayerNorm}(\mathbf{X} + \text{Attention}(\mathbf{X}\mathbf{W}_Q, \mathbf{Y}\mathbf{W}_K, \mathbf{Y}\mathbf{W}_V)), \quad \mathbf{G}''_q = \mathbf{S}, \quad (11)$$

where  $\mathbf{G} \in \mathbb{R}^{(m*k)*3d}$  is the stacked result of the  $m$  input embedding and  $\text{AttentionBlock}(\cdot)$  is a permutation equivariant set attention block network.  $\text{PoolingAttention}_k(\cdot)$  is a pooling attention

network with  $k$  seed vectors, which can adaptively aggregate intersection information from the output of self-attention network.  $\mathbf{S} \in \mathbb{R}^{k \times 3d}$  is a set of  $k$  learnable seed vectors, also, the attention pooling result  $\mathbf{G}_q''$ .

Last, to effectively combine the results of both the inter-query level and the inter-subset level, we employ a gating mechanism to fuse the information of the two parts:

$$\mathbf{g}_t = \sigma(\mathbf{W}_{g_t}(\mathbf{G}_q' \oplus \mathbf{G}_q'')), \quad \mathbf{G}_q = \mathbf{g}_t \mathbf{G}_q' + (1 - \mathbf{g}_t) \mathbf{G}_q'' \quad (12)$$

where  $\oplus$  denotes the concatenation of the input matrix. By Eq. (12), we can obtain the final output result by leveraging two-levels interaction learning.

### 3.4 Negation

Given a GMM embedding of an entity set, the aim of the negation operator is to identify the complementary set of the given entity set according to the global cross-correlation among the components of the input entity set (see Fig. 2c). Thus, we utilize a self-attention block layer [26] while excluding the positional encoding, to learn the global correlation among these subsets. We model the negation operator as follows:

$$\tilde{\mathbf{G}}_{-q} = \text{Attention}(\mathbf{G}_q \mathbf{W}_Q, \mathbf{G}_q \mathbf{W}_K, \mathbf{G}_q \mathbf{W}_V), \quad \tilde{\mathbf{G}}_{-q} = \text{LayerNorm}(\mathbf{G}_q + \tilde{\mathbf{G}}_{-q}), \quad (13)$$

$$\mathbf{G}_{-q} = \text{LayerNorm}(\tilde{\mathbf{G}}_{-q} + \text{rFF}(\tilde{\mathbf{G}}_{-q})), \quad (14)$$

where  $\mathbf{W}_Q \in \mathbb{R}^{3d \times 3d}$ ,  $\mathbf{W}_K \in \mathbb{R}^{3d \times 3d}$  and  $\mathbf{W}_V \in \mathbb{R}^{3d \times 3d}$  are learnable parameters.  $\text{rFF}(\cdot)$  refers to a row-wise feedforward layer. By Eq. (13), each subset of the input entity set is aware of the global answer areas. We then encourage the embedding of each sub-distribution to shift towards the areas that are not covered by the given entity set based on Eq. (14).

### 3.5 Union

Given a query  $q$ , the goal of the union operator is to cover all answer entities from all input entity sets (see Fig. 2d). In Query2GMM, it is natural to model the union of multiple entity sets based on the Gaussian mixture distribution without extra transformation for the computation graph. Interestingly, based on our initial experiments, we have found that it is more effective to use the DNF technique [18] for union operation. Thus, we transform the union operator to the end of the computation graph and directly use the union of the final multiple solution sets as the output. It is worth noting that the additional cost of query transformation can be alleviated through parallel computation of the conjunctive sub-queries.

### 3.6 Learning GMM Embeddings

**Similarity measurement.** In the reasoning process, we expect that the answer entities should be close to the query. To achieve this, given the Gaussian embedding  $\mathbf{G}_e = [\boldsymbol{\mu}_e; \boldsymbol{\sigma}_e]$  of an entity and the GMM embedding  $\mathbf{G}_q = [[\boldsymbol{\alpha}_1; \boldsymbol{\mu}_1; \boldsymbol{\sigma}_1], \dots, [\boldsymbol{\alpha}_k; \boldsymbol{\mu}_k; \boldsymbol{\sigma}_k]]$  of the target node of the query, we need to measure the similarity between the entity and the query, which serves as the foundation in multi-modal distribution modelling for our Query2GMM.

Actually, there is no existing feasible solution to compute the similarity between the Gaussian distribution and the Gaussian mixture distribution, but the literature [29] proposes to repeat the Gaussian distribution  $k$  times identically to generate an equally Gaussian mixture distribution, then the original problem can be transformed into the calculation paradigm for Kullback-Leibler (KL) divergence between Gaussian mixture distributions. However, the Kullback-Leibler divergence of Gaussian mixture distributions is not analytically tractable [30]. Fortunately, we can use the upper bound to approximately minimize the KL divergence between Gaussian mixture distributions based on the following Theorem.

**Theorem 1** Given two Gaussian mixture distributions  $p_1 = \sum_{i=1}^k \alpha_i^1 \phi(\mu_i^1, \sigma_i^1)$  and  $p_2 = \sum_{i=1}^k \alpha_i^2 \phi(\mu_i^2, \sigma_i^2)$ , their Kullback-Leibler divergence is bounded by  $D_{KL}[p_1||p_2] \leq D_{KL}[\alpha^1||\alpha^2] + \sum_{i=1}^k \alpha_i^1 D_{KL}[\phi(\mu_i^1, \sigma_i^1)||\phi(\mu_i^2, \sigma_i^2)]$ , with equality if and only if  $\frac{\alpha_i^1 \phi(\mu_i^1, \sigma_i^1)}{\sum_{i=1}^k \alpha_i^1 \phi(\mu_i^1, \sigma_i^1)} = \frac{\alpha_i^2 \phi(\mu_i^2, \sigma_i^2)}{\sum_{i=1}^k \alpha_i^2 \phi(\mu_i^2, \sigma_i^2)}$  for  $\forall i$ .

The proof is provided in [31]. Based on Theorem 1, the upper bound of the KL divergence between a Gaussian distribution  $p_e$  and a Gaussian mixture distribution  $p_q$  can be defined as

$$\begin{aligned} D_{KL}[p_e||p_q] &\leq \sum_i^k \alpha_i^e \log \frac{\alpha_i^e}{\alpha_i^q} + \sum_i^k \alpha_i^e D_{KL}[\phi(\mu_i^e, \sigma_i^e)||\phi(\mu_i^q, \sigma_i^q)] \\ &= \sum_i^k \frac{1}{k} \log \frac{1}{k \alpha_i^q} + \sum_i^k \frac{1}{k} D_{KL}[\phi(\mu_i^e, \sigma_i^e)||\phi(\mu_i^q, \sigma_i^q)]. \end{aligned} \quad (15)$$

KL divergence is inherently asymmetric. Nonetheless, our task requires bidirectional adjustments for queries and answer entities to establish many-to-many mapping relationships, which is hard to be implemented through the KL divergence. Moreover, KL divergence fails to measure the distance between distributions when the input distributions do not intersect. To solve these issues, we define a new similarity function (named mixed Wasserstein distance), based on the Wasserstein distance [22] and the upper bound of KL divergence, to compute the distance between Gaussian distribution and Gaussian mixture distribution. Concretely, we replace the  $D_{KL}[\phi(\mu_i^e, \sigma_i^e)||\phi(\mu_i^q, \sigma_i^q)]$  in Eq. (15) with the Wasserstein distance (p=2) [32] and then we obtain

$$D_{\text{mix}}[p_e||p_q] = \sum_i^k \frac{1}{k} \log \frac{1}{k \alpha_i^q} + \sum_i^k \frac{1}{k} D_{WD}[\phi(\mu_i^e, \sigma_i^e)||\phi(\mu_i^q, \sigma_i^q)]. \quad (16)$$

Here,  $D_{WD}[\phi(\mu_i^e, \sigma_i^e)||\phi(\mu_i^q, \sigma_i^q)] = \sqrt{\|\mu_i^e - \mu_i^q\|_2^2 + \|\sigma_i^e - \sigma_i^q\|_2^2}$  is the Wasserstein distance. Furthermore, given the Gaussian embedding  $\mathbf{G}_e$  of an entity and the GMM embedding  $\mathbf{G}_q$  of a query, the mixed Wasserstein distance between an entity and the query can be defined as the sum of distribution distance along each dimension:

$$D_{\text{mix}}(\mathbf{G}_e; \mathbf{G}_q) = \sum_{j=1}^d D_{\text{mix}}[p_{e,j}||p_{q,j}]. \quad (17)$$

Therefore, we can compute the relationships between entities and queries by our proposed mixed Wasserstein distance  $D_{\text{mix}}(\cdot)$  in Eq. (17). This serves as the foundation for multi-modal distribution modelling in logical reasoning.

**Training Objective.** To minimize the distance between the GMM embedding of the query and the Gaussian embeddings of its answer entities, we take the normalized probability of an entity  $e$  being the correct answer of the query  $q$  by using the Softmax function on all similarity scores. To be specific, we compute the reciprocal of the distance function as the similarity score [32]. Following Query2Particles [6], we also use cross-entropy loss constructed from the given probabilities. The loss function aims to maximize the log probabilities of all correct query-answer pairs:

$$L = -\frac{1}{M} \sum_{t=1}^M \log \text{Prob}(e^t, q), \quad \text{Prob}(e, q) = \frac{\exp(1/D_{\text{mix}}(\mathbf{G}_e; \mathbf{G}_q))}{\sum_{e' \in V} \exp(1/D_{\text{mix}}(\mathbf{G}_{e'}; \mathbf{G}_q))}, \quad (18)$$

where  $M$  is the amount of ground-truth answer entities.

**Remarks.** Notably, existing works [4, 10] utilize multivariate Gaussian distribution to learn the query embedding, there are major differences between our Query2GMM and them: (1) Fundamentally, only Query2GMM is capable of learning diversified answers with multi-modal distribution in the reasoning process. This is done through our design and the proposed mixed Wasserstein distance.

Table 1: MRR results (%) for answering queries on three KGs.  $A_p$  and  $A_n$  represent the average score of EPFO queries and queries with negation, respectively. The best result is highlighted in bold.

KG	Model	Query														$A_p$	$A_n$
		1p	2p	3p	2i	3i	ip	pi	2u	up	2in	3in	inp	pin	pni		
FB15k	BetaE	64.1	25.2	24.7	55.1	66.0	27.6	43.4	39.8	24.9	14.0	14.6	11.5	6.3	12.4	41.2	11.8
	PERM	72.6	32.9	27.5	56.9	68.3	25.9	40.7	52.3	24.7	-	-	-	-	-	44.6	-
	NMP-QEM	76.4	35.9	30.3	54.2	65.9	23.6	42.0	55.8	25.3	16.9	17.6	11.0	7.9	15.2	45.5	13.7
	Q2P	80.4	46.1	39.8	64.1	72.9	22.4	43.7	65.4	27.9	21.9	20.8	12.5	8.9	17.1	51.4	16.4
	LMPNN	85.0	39.3	28.6	<b>68.2</b>	76.5	<b>43.0</b>	<b>46.7</b>	36.7	<b>31.4</b>	<b>29.1</b>	<b>29.4</b>	<b>14.9</b>	10.2	16.4	50.6	<b>20.0</b>
	Ours	<b>88.7</b>	<b>53.9</b>	<b>45.4</b>	67.6	<b>76.8</b>	27.5	43.2	<b>69.0</b>	28.7	27.0	27.5	14.5	<b>10.8</b>	<b>19.5</b>	<b>55.7</b>	19.9
FB237	BetaE	38.9	10.7	9.8	29.1	42.4	12.0	22.3	11.9	9.9	4.8	7.9	7.4	3.4	3.3	20.8	5.4
	PERM	42.4	23.9	18.6	27.5	37.6	11.8	20.3	19.4	10.7	-	-	-	-	-	23.6	-
	NMP-QEM	44.7	17.8	13.8	32.5	43.6	11.5	22.9	17.3	12.5	5.8	9.7	7.2	4.4	3.7	24.1	6.2
	Q2P	36.7	25.7	22.7	28.7	43.7	11.4	20.2	19.2	16.9	4.4	9.7	7.5	4.6	3.8	25.0	6.0
	LMPNN	45.9	13.1	10.3	34.8	48.9	<b>17.6</b>	22.7	13.5	10.3	<b>8.7</b>	12.9	7.7	4.6	<b>5.2</b>	24.1	7.8
	Ours	<b>46.3</b>	<b>28.3</b>	<b>23.2</b>	<b>35.8</b>	<b>50.5</b>	11.1	<b>23.3</b>	<b>23.8</b>	<b>18.2</b>	8.6	<b>15.3</b>	<b>9.3</b>	<b>6.1</b>	4.3	<b>28.9</b>	<b>8.7</b>
NELL	BetaE	53.7	13.4	11.6	37.6	48.2	15.5	24.7	12.4	9.2	5.2	7.5	10.1	3.1	3.2	25.1	5.8
	PERM	45.2	20.4	17.7	29.6	43.8	12.2	17.8	30.2	18.0	-	-	-	-	-	26.1	-
	NMP-QEM	52.2	23.7	18.9	33.4	44.1	15.8	20.9	22.8	13.7	4.8	8.2	9.3	3.8	3.5	27.3	5.9
	Q2P	54.3	28.8	29.3	29.4	45.4	10.9	18.1	36.8	19.5	5.1	7.4	10.2	3.3	3.4	30.3	6.0
	LMPNN	60.6	22.1	17.5	<b>40.1</b>	50.3	<b>24.9</b>	<b>28.4</b>	17.2	15.7	8.5	10.8	12.2	3.9	4.8	30.7	8.0
	Ours	<b>63.1</b>	<b>35.6</b>	<b>33.3</b>	39.8	<b>54.7</b>	16.1	25.7	<b>45.7</b>	<b>21.4</b>	<b>9.0</b>	<b>12.9</b>	<b>14.3</b>	<b>5.3</b>	<b>5.7</b>	<b>37.3</b>	<b>9.4</b>

However, existing works do not. (2) Different from them, Query2GMM takes the Cartesian product for the embedding representation based on univariate Gaussian (mixture) distribution. This maintains the linear complexity of the model and avoids complicated computation, e.g., the inverse of the covariance matrix. (3) We design more effective neural models for logical operators considering their own properties in the multi-modal distribution context. This helps handle complex mapping relationships and alleviates cascading errors.

## 4 Experiments

### 4.1 Experimental Settings

**Datasets and Baselines.** We evaluate the proposed Query2GMM on three commonly-used standard knowledge graphs: FB15k [33], FB15k-237(FB237) [34] and NELL995(NELL) [35]. We consider five baselines as the compared methods, covering the uni-modal based models (BetaE [11], PERM [4]), multi-modal based models (NMP-QEM [10], Q2P [6]) and pre-trained based model (LMPNN [16]).

**Training Protocol.** We implement Query2GMM in Pytorch on Nvidia RTX 3090 GPU. And we set embedding dimension  $d$  as 400. We use the uniform distribution for the parameter initialization. Additionally, we utilize grid search for hyperparameter tuning. The learning rate varies between 0.0001 and 0.001, and the batch size ranges from 512 to 8192.

### 4.2 Reasoning over Knowledge Graphs

To evaluate the quality of query embedding, we compare our Query2GMM with five baselines. Following [18, 11], we use fourteen types of queries based on the first-order logic queries and report Mean Reciprocal Rank (MRR) results on three datasets. Due to the space limitation, we report more results in the Supplementary.

We can observe from Table. 1 that (1) Our Query2GMM significantly outperforms all baselines in most cases. This underlines the effectiveness of our proposed embedding backbone (i.e., GMM embedding), coupled with our neural operators, in accurately representing complex logical queries. (2) Multi-modal based models (NMP-QEM, Q2P, and Query2GMM) demonstrate better empirical performance compared to uni-modal based models (BetaE and PERM), implying that they are more adept at fitting diverse answers. (3) Compared to NMP-QEM, which uses a multivariate Gaussian mixture distribution for the query embedding, Query2GMM shows an overall average improvement of 12.4%. Despite NMP-QEM’s initial structure following a multi-modal distribution, it tends to default to uni-modal distribution modelling during the reasoning process, which diminishes its reasoning performance. This emphasizes the crucial role of reasoning within the multi-modal distribution learning framework. Our proposed mixed Wasserstein distance forms the foundation of



Table 2: Ablation study on NELL regarding MRR score. The best result is highlighted in bold.

Method	Query									
	1p	2p	3p	2i	3i	ip	pi	2u	up	Average
Query2GMM	<b>63.1</b>	<b>35.6</b>	<b>33.3</b>	<b>39.8</b>	<b>54.7</b>	<b>16.1</b>	<b>25.7</b>	<b>45.7</b>	<b>21.4</b>	<b>37.3</b>
w/o Cardinality	60.2	33.8	32.2	35.2	51.1	14.2	22.1	41.6	19.2	34.4
w/o Dispersion	60.7	35.0	31.7	36.2	52.3	14.8	22.7	41.2	19.5	34.9
Query2GMM <sub>pro</sub>	58.7	32.7	31.4	-	-	7.4	18.1	-	19.2	-
Query2GMM <sub>inter</sub>	-	-	-	32.6	42.5	14.2	19.4	-	-	-

this process, demonstrating its effectiveness in handling complex logical queries. (4) The performance of complex logical queries can be enhanced by accurately representing multiple subsets, as shown in the comparison between Query2GMM and Q2P. We will provide more detailed benefits in the following subsection. (5) Compared to LMPNN using pre-trained techniques, our Query2GMM achieves better performance in most cases, showing the effectiveness of multi-subset modelling in answering complex logical queries; meanwhile, Query2GMM performs relatively inferior on some queries with intersection operator. This is because, in the multi-modal distribution context, the complexity of intersection relationships increases  $k$ -fold. In these cases, Query2GMM beats multi-modal based baselines by considering two-level intersections.

### 4.3 Ablation Study

In the ablation study, we conduct extensive experiments to justify the effects of four key components of Query2GMM, including (1) the cardinality of GMM embedding, (2) the dispersion degree of GMM embedding, (3) the proposed neural projection operator and (4) the proposed neural intersection operator. Here, all experiments are conducted on queries on the NELL dataset in terms of MRR.

To justify the effect of our GMM embedding, we conduct two variants "w/o Cardinality" and "w/o Dispersion" by removing the cardinality parameter and dispersion degree parameter, respectively. As shown in Table. 2, cardinality and dispersion degree play individual and important roles in accurate representation for query embedding in the multi-modal distribution context, achieving an average improvement of 2.9% and 2.4%, respectively. This suggests that the effectiveness of multi-modal distribution modelling for logical queries relies on three elements: cardinality, semantic center and degree of dispersion.

Additionally, we replace our neural model with 3-layer MLPs for the projection operator, called Query2GMM<sub>pro</sub>. The performance of Query2GMM<sub>pro</sub> drops up to 8.7%, affirming the effectiveness of our proposed model: independent component learning based on gate mechanism, in conjunction with joint learning using the self-attention mechanism.

Furthermore, we replace our neural model with self-attention and random sampling used in Q2P [6] for the intersection operator, called Query2GMM<sub>inter</sub>. The performance falls by up to 12.2%, showing that effectively modelling at the inter-query and inter-subset levels can more accurately adapt to the complex mapping relationships inherent in intersection operations. Meanwhile, our proposed co-attention model can adaptively generate results, thereby facilitating the coverage of  $m$ -intersected answer areas in the multi-modal distribution context. We also provide other ablation results in the Supplementary.

## 5 Related Works

Answering complex logical queries is one of the long-standing topics in reasoning on knowledge graphs. The existing works can be broadly grouped into subgraph-based [36, 37, 38] and embedding-based methods [27, 6, 33, 7, 8, 9, 10, 19, 11, 21, 12, 39, 13, 20, 14, 15, 16, 17]. Since real-life KGs are typically incomplete, embedding-based methods achieve promising performance in answering logical queries over incomplete KGs. Along this line, most existing methods can be classified into two groups: uni-modal based models and multi-modal based models. The former [12, 8, 11, 18, 40] based on a strong assumption inevitably introduces more false positive answers, violating the semantics of

query embeddings and then degrading the performance, as it is validated in the literature [6, 10] and our experiments. The latter [6, 10] attempts to model the ideal distribution of answer entities, but they struggle to accurately characterize each subset of an answer set for each query. Even one [10] fails to evaluate the relationships between an entity and multiple subsets of a query, leading to multi-modal distribution modelling degenerating into uni-modal distribution modelling during the reasoning process. Moreover, our experiments in Section. 4.3 suggest that accurate subset representation is essential for answering logical queries.

## 6 Conclusion

In this paper, we investigate the multi-modal distribution of answers for each query in logical reasoning over knowledge graphs. To achieve this, we propose Query2GMM, a query embedding method for complex logical query answering. Unlike existing works, Query2GMM is able to elegantly and accurately represent each subset using cardinality, semantic center and dispersion degree with the proposed GMM embedding. Furthermore, we define a new mixed Wasserstein distance to measure the relationships between an entity and multiple answer subsets. This provides a solid foundation for reasoning within multi-modal distribution learning. Extensive experiments demonstrate the effectiveness of our proposed Query2GMM and each of its key components. Crucially, we empirically observe that modelling the multi-modal distribution during the reasoning process is of greater importance than the initial representation for complex logical query answering.

## References

- [1] H. Ren, H. Dai, B. Dai, X. Chen, M. Yasunaga, H. Sun, D. Schuurmans, J. Leskovec, and D. Zhou, “LEGO: latent execution-guided reasoning for multi-hop question answering on knowledge graphs,” in *Proceedings of the International Conference on Machine Learning*, vol. 139. PMLR, 2021, pp. 8959–8970.
- [2] F.-L. Li, M. Qiu, H. Chen, X. Wang, X. Gao, J. Huang, J. Ren, Z. Zhao, W. Zhao, L. Wang *et al.*, “Alime assist: An intelligent assistant for creating an innovative e-commerce experience,” in *Proceedings of the ACM on Conference on Information and Knowledge Management*, 2017, pp. 2495–2498.
- [3] L. Li, P. Wang, J. Yan, Y. Wang, S. Li, J. Jiang, Z. Sun, B. Tang, T. Chang, S. Wang, and Y. Liu, “Real-world data medical knowledge graph: construction and applications,” *Artif. Intell. Medicine*, vol. 103, p. 101817, 2020.
- [4] N. Choudhary, N. Rao, S. Katariya, K. Subbian, and C. Reddy, “Probabilistic entity representation model for reasoning over knowledge graphs,” *Advances in Neural Information Processing Systems*, vol. 34, pp. 23 440–23 451, 2021.
- [5] S. Ji, S. Pan, E. Cambria, P. Martinen, and P. S. Yu, “A survey on knowledge graphs: Representation, acquisition, and applications,” *IEEE Trans. Neural Networks Learn. Syst.*, vol. 33, no. 2, pp. 494–514, 2022.
- [6] J. Bai, Z. Wang, H. Zhang, and Y. Song, “Query2particles: Knowledge graph reasoning with particle embeddings,” *Proceedings of the Findings of the Association for Computational Linguistics: NAACL*, pp. 2703–2714, 2022.
- [7] W. Hamilton, P. Bajaj, M. Zitnik, D. Jurafsky, and J. Leskovec, “Embedding logical queries on knowledge graphs,” *Advances in neural information processing systems*, vol. 31, 2018.
- [8] N. Choudhary, N. Rao, S. Katariya, K. Subbian, and C. K. Reddy, “Self-supervised hyperboloid representations from logical queries over knowledge graphs,” in *Proceedings of the Web Conference*, 2021, pp. 1373–1384.
- [9] Z. Huang, M.-F. Chiang, and W.-C. Lee, “Line: Logical query reasoning over hierarchical knowledge graphs,” in *Proceedings of the ACM SIGKDD Conference on Knowledge Discovery and Data Mining*, 2022, pp. 615–625.
- [10] X. Long, L. Zhuang, L. Aodi, S. Wang, and H. Li, “Neural-based mixture probabilistic query embedding for answering fol queries on knowledge graphs,” in *Proceedings of the Conference on Empirical Methods in Natural Language Processing*, 2022, pp. 3001–3013.

- [11] H. Ren and J. Leskovec, “Beta embeddings for multi-hop logical reasoning in knowledge graphs,” *Advances in Neural Information Processing Systems*, vol. 33, pp. 19 716–19 726, 2020.
- [12] Z. Zhang, J. Wang, J. Chen, S. Ji, and F. Wu, “Cone: Cone embeddings for multi-hop reasoning over knowledge graphs,” *Advances in Neural Information Processing Systems*, vol. 34, pp. 19 172–19 183, 2021.
- [13] H. Sun, A. Arnold, T. Bedrax Weiss, F. Pereira, and W. W. Cohen, “Faithful embeddings for knowledge base queries,” *Advances in Neural Information Processing Systems*, vol. 33, pp. 22 505–22 516, 2020.
- [14] Z. Hu, V. Gutiérrez-Basulto, Z. Xiang, X. Li, R. Li, and J. Z. Pan, “Type-aware embeddings for multi-hop reasoning over knowledge graphs,” in *Proceedings of the International Joint conference on Artificial Intelligence*, 2022.
- [15] Z. Xu, W. Zhang, P. Ye, H. Chen, and H. Chen, “Neural-symbolic entangled framework for complex query answering,” in *Advances in Neural Information Processing Systems*, 2022.
- [16] Z. Wang, Y. Song, G. Wong, and S. See, “Logical message passing networks with one-hop inference on atomic formulas,” in *Proceedings of The International Conference on Learning Representations (ICLR)*, 2023.
- [17] A. Amayuelas, S. Zhang, S. X. Rao, and C. Zhang, “Neural methods for logical reasoning over knowledge graphs,” in *Proceedings of The International Conference on Learning Representations*. OpenReview.net, 2022.
- [18] H. Ren, W. Hu, and J. Leskovec, “Query2box: Reasoning over knowledge graphs in vector space using box embeddings,” in *Proceedings of the International Conference on Learning Representations*. OpenReview.net, 2020.
- [19] X. Liu, S. Zhao, K. Su, Y. Cen, J. Qiu, M. Zhang, W. Wu, Y. Dong, and J. Tang, “Mask and reason: Pre-training knowledge graph transformers for complex logical queries,” in *Proceedings of the ACM SIGKDD Conference on Knowledge Discovery and Data Mining*, 2022, pp. 1120–1130.
- [20] E. Arakelyan, D. Daza, P. Minervini, and M. Cochez, “Complex query answering with neural link predictors,” in *Proceedings of the International Conference on Learning Representations*. OpenReview.net, 2021.
- [21] G. Wan, S. Pan, C. Gong, C. Zhou, and G. Haffari, “Reasoning like human: Hierarchical reinforcement learning for knowledge graph reasoning,” in *Proceedings of the international conference on international joint conferences on artificial intelligence*, 2021, pp. 1926–1932.
- [22] L. Rüschendorf, “The wasserstein distance and approximation theorems,” *Probability Theory and Related Fields*, vol. 70, no. 1, pp. 117–129, 1985.
- [23] X. Wu and J. M. Perloff, “Gmm estimation of a maximum entropy distribution with interval data,” *Journal of Econometrics*, vol. 138, no. 2, pp. 532–546, 2007.
- [24] M. Ravanelli, P. Brakel, M. Omologo, and Y. Bengio, “Light gated recurrent units for speech recognition,” *IEEE Transactions on Emerging Topics in Computational Intelligence*, vol. 2, no. 2, pp. 92–102, 2018.
- [25] J. L. Ba, J. R. Kiros, and G. E. Hinton, “Layer normalization,” *arXiv preprint arXiv:1607.06450*, 2016.
- [26] A. Vaswani, N. Shazeer, N. Parmar, J. Uszkoreit, L. Jones, A. N. Gomez, Ł. Kaiser, and I. Polosukhin, “Attention is all you need,” *Advances in neural information processing systems*, vol. 30, 2017.
- [27] K. Guu, J. Miller, and P. Liang, “Traversing knowledge graphs in vector space,” *Proceedings of the Conference on Empirical Methods in Natural Language Processing*, pp. 318–327, 2015.
- [28] J. Lee, Y. Lee, J. Kim, A. Kosiorek, S. Choi, and Y. W. Teh, “Set transformer: A framework for attention-based permutation-invariant neural networks,” in *International conference on machine learning*. PMLR, 2019, pp. 3744–3753.
- [29] F. Nielsen and K. Sun, “Guaranteed bounds on the kullback-leibler divergence of univariate mixtures using piecewise log-sum-exp inequalities,” *Entropy*, vol. 18, no. 12, p. 442, 2016.
- [30] S. Watanabe, “Kullback information of normal mixture is not an analytic function,” *IEICE Technical Report*, vol. 2004, pp. 41–46, 2004.

- [31] T. M. Cover, *Elements of information theory*. John Wiley & Sons, 1999.
- [32] J. Zhang, W. Zhou, X. Chen, W. Yao, and L. Cao, “Multisource selective transfer framework in multiobjective optimization problems,” *IEEE Transactions on Evolutionary Computation*, vol. 24, no. 3, pp. 424–438, 2019.
- [33] A. Bordes, N. Usunier, A. Garcia-Duran, J. Weston, and O. Yakhnenko, “Translating embeddings for modeling multi-relational data,” *Advances in neural information processing systems*, vol. 26, 2013.
- [34] K. Toutanova and D. Chen, “Observed versus latent features for knowledge base and text inference,” in *Proceedings of the workshop on continuous vector space models and their compositionality*, 2015, pp. 57–66.
- [35] W. Xiong, T. Hoang, and W. Y. Wang, “Deeppath: A reinforcement learning method for knowledge graph reasoning,” pp. 564–573, 2017.
- [36] H. Tong, C. Faloutsos, B. Gallagher, and T. Eliassi-Rad, “Fast best-effort pattern matching in large attributed graphs,” in *Proceedings of the ACM SIGKDD International Conference on Knowledge Discovery and Data Mining*. ACM, 2007, pp. 737–746.
- [37] B. Du, S. Zhang, N. Cao, and H. Tong, “FIRST: fast interactive attributed subgraph matching,” in *Proceedings of the ACM SIGKDD International Conference on Knowledge Discovery and Data Mining*. ACM, 2017, pp. 1447–1456.
- [38] L. Liu, B. Du, J. Xu, and H. Tong, “G-finder: Approximate attributed subgraph matching,” in *Proceedings of the IEEE International Conference on Big Data*. IEEE, 2019, pp. 513–522.
- [39] R. Das, A. Neelakantan, D. Belanger, and A. McCallum, “Chains of reasoning over entities, relations, and text using recurrent neural networks,” pp. 132–141, 2017.
- [40] L. Liu, B. Du, H. Ji, C. Zhai, and H. Tong, “Neural-answering logical queries on knowledge graphs,” in *Proceedings of the ACM SIGKDD conference on knowledge discovery & data mining*, 2021, pp. 1087–1097.
- [41] P. Indyk and R. Motwani, “Approximate nearest neighbors: Towards removing the curse of dimensionality,” in *Proceedings of the Thirtieth Annual ACM Symposium on the Theory of Computing, Dallas*. ACM, 1998, pp. 604–613.

## A Additional Technical Details on Query2GMM

### A.1 Co-attention Network for Intersection Operator

When modelling the query embedding with multi-modal distribution, Query2GMM is capable of fitting the ideal distribution of the ground-truth answer set while introducing as few false positives as possible. Meanwhile, the complexity of the intersection operator increases  $k$ -fold ( $k$ -modal distribution). To cope with this, we design a co-attention network to capture both inter-query and inter-subset level information for the  $m$ -intersected regions. Fig. 3 illustrates the procedure of our co-attention network. For the inter-query level, we capture cross-correlation information of  $m$  GMM embeddings by employing a cross-attention network. For the inter-subset level, we obtain the global cross correlation between  $m * k$  sub-distributions using the self-attention network [26]. To fit the output with  $k$  sub-distributions, we use attention pooling [28] to adaptively generate the output of the inter-subset level. To effectively combine the information from two levels, a gate mechanism  $g_t$  is used to synthesize the information of the two parts to get the final intersected output.

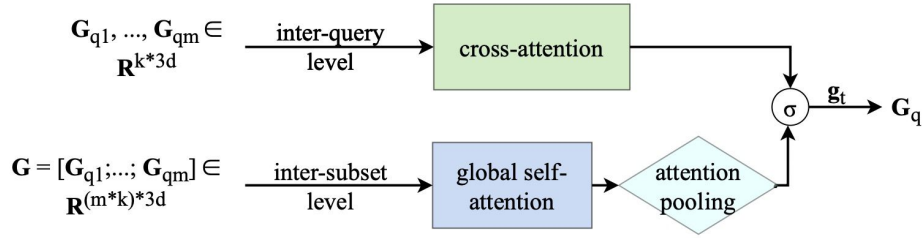


Figure 3: Co-attention model for intersection operator.

### A.2 Proof of Theorem 1

With non negative real numbers  $a_1, a_2, \dots, a_n$  and  $b_1, b_2, \dots, b_n$ , the following log-sum inequality [31] holds:

$$\sum_{i=1}^n a_i \log \frac{a_i}{b_i} \geq \left( \sum_{i=1}^n a_i \right) \log \frac{\sum_{i=1}^n a_i}{\sum_{i=1}^n b_i}, \quad (19)$$

thus the upper bound of the KL distance between two univariate Gaussian mixture distributions is given by

$$\begin{aligned} D_{KL}[p_1||p_2] &= \int \left( \sum_i \alpha_i^1 \phi(\mu_i^1, \sigma_i^1) \right) \log \frac{\sum_i \alpha_i^1 \phi(\mu_i^1, \sigma_i^1)}{\sum_i \alpha_i^2 \phi(\mu_i^2, \sigma_i^2)}, \\ &\leq \int \sum_i \alpha_i^1 \phi(\mu_i^1, \sigma_i^1) \log \frac{\alpha_i^1 \phi(\mu_i^1, \sigma_i^1)}{\alpha_i^2 \phi(\mu_i^2, \sigma_i^2)}, \\ &= \sum_i \alpha_i^1 \log \frac{\alpha_i^1}{\alpha_i^2} \int \phi(\mu_i^1, \sigma_i^1) + \sum_i \alpha_i^1 \int \phi(\mu_i^1, \sigma_i^1) \log \frac{\phi(\mu_i^1, \sigma_i^1)}{\phi(\mu_i^2, \sigma_i^2)}, \\ &= \sum_i \alpha_i^1 \log \frac{\alpha_i^1}{\alpha_i^2} + \sum_i \alpha_i^1 D_{KL}[\phi(\mu_i^1, \sigma_i^1)||\phi(\mu_i^2, \sigma_i^2)]. \end{aligned} \quad (20)$$

### A.3 Overview of Query2GMM

The overall learning of our proposed Query2GMM is composed of the offline stage for training and the online stage for testing. For the training stage, given the input query-answer pairs, we first construct the corresponding computation graph. We treat the computation graph as a sequence of logical operations and model each logical operation as a neural network. Then we learn Gaussian

---

**Algorithm 1:** Query2GMM Algorithm

---

**Input:** Queries  $Q$  with positive ground-truth entities  $V_p$ , knowledge graph triples;

**Output:** Entity Gaussian embeddings, relation Gaussian embeddings;

```
1 Initialize  $G_e \in E, G_r \in R$ ;  
2 while  $t \leq \text{MaxStep}$  or not convergence do  
3   for batch query with the same structure  $\in Q$  do  
4     loss = 0;  
5     Look up the Gaussian embeddings of anchor entities and relations;  
6     Get the corresponding GMM embeddings  $G_q$  by expanding the Gaussian embeddings of  
       anchor entities by Eq.(3);  
7     while ( $op = \text{nextOp}(\cdot) \neq \text{NULL}$ ) do  
8       if  $op == \text{'projection'}$  then  
9         Compute the result GMM embedding  $G'_q$  by Eq.(4)-(6);  
10      if  $op == \text{'intersection'}$  then  
11        Compute the result GMM embedding  $G'_q$  by Eq.(7)-(12);  
12      if  $op == \text{'negation'}$  then  
13        Compute the result GMM embedding  $G'_q$  by Eq.(13)-(14);  
14      if  $op == \text{'union'}$  then  
15        Union of  $m$  input GMM embeddings;  
16      Compute the loss according to Eq.(18);  
17       $t += 1$ ;  
18 return  $E$  and  $R$ .
```

---

embeddings for entities and relations over the knowledge graph  $G$ , and the parameterized neural networks for all the logical operators simultaneously until the convergence of the model.

For the online stage, the trained model serves as generating the GMM embedding for the target node of the test logical query by executing a set of logical operations. With the target GMM embedding, we measure the similarity between entities and the query according to the mixed Wasserstein distance between them in the embedding space. Last, the top- $k$  entities will be selected as answers to the query. The procedure of our Query2GMM is given in Algorithm 1.

#### A.4 Computational Complexity

The computational complexity of answering a logical query simply involves processing the  $n$  conjunctive queries after DNF transformation [18]. Note that all  $n$  computations can be tackled in parallel. And the execution time for each conjunctive query is essentially an aggregate of the execution times for the operators within it, which is typically the constant time. To get the final answers, we perform a range search in the low-dimensional vector, which can also be done in constant time using the search algorithms, such as Locality Sensitive Hashing (LSH) [41]. In summary, processing a logical query online is fast. Meanwhile, the online time will not significantly increase as the knowledge graphs/queries gradually expand.

## B Additional Experimental Results

### B.1 Datasets and Queries

Table. 3 presents the statistics of datasets used in our experiments. For each dataset, we create three graphs respectively for training, validation and testing, which satisfies  $\mathcal{G}_{\text{training}} \subseteq \mathcal{G}_{\text{validation}} \subseteq \mathcal{G}_{\text{testing}}$ . Here,  $\mathcal{G}_{\text{training}}$  contains *training* edges is the training graph for the learning of entity embeddings, relation embeddings, neural networks of logical operators and other learnable parameters.  $\mathcal{G}_{\text{validation}}$  includes  $\mathcal{G}_{\text{training}}$  plus the *validation* edges and  $\mathcal{G}_{\text{testing}}$  is the biggest graph among them, including  $\mathcal{G}_{\text{validation}}$  as well as the *testing* edges.

Table 3: Statistics of three benchmark datasets, where nodes denote entities and edges represent relations in the KGs.

Dataset	Entities	Relations	Training Edges	Validation Edges	Testing Edges	Total Edges
FB15k	14,951	1,345	483,142	50,000	59,071	592,213
FB237	14,505	237	272,115	17,526	20,438	310,079
NELL	63,361	200	114,213	14,324	14,267	142,804

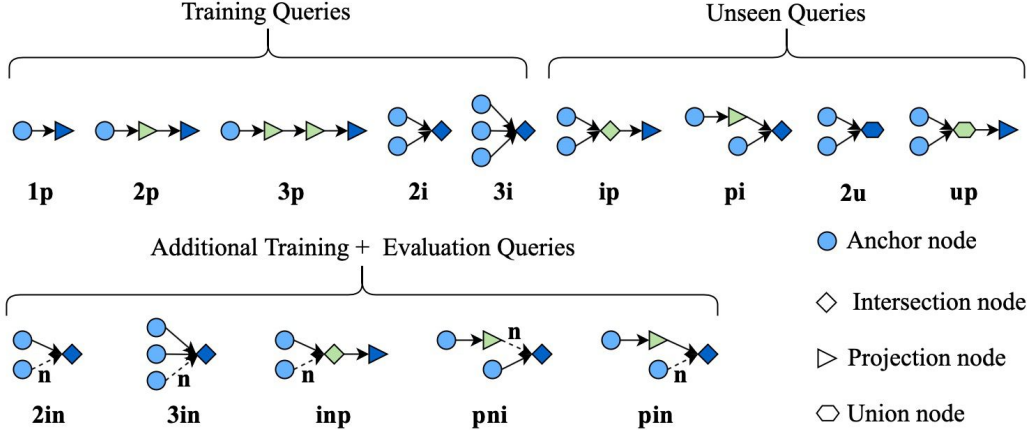


Figure 4: Query structures with the abbreviation of their computation graph used in the experiments, where 'p', 'i', 'u', and 'n' represent 'projection', 'intersection', 'union', and 'negation'.

In our experiments, we employ 14 different types of query structures, as illustrated in Fig. 4. The query structures displayed on the top row serve to evaluate performance when answering Existential Positive First-Order (EPFO) queries. Some of them, namely 'ip', 'pi', '2u', and 'up', are only used for the validation and testing phases to assess the generalization capability of comparable methods. The additional query structures on the bottom row, in conjunction with those from the top row, are employed to analyze the model's effectiveness in handling queries with the negation operator (i.e., negative queries).

## B.2 Additional Reasoning Results

We provide supplementary results on three knowledge graphs in terms of Hit@3 and Hit@10. Tables 4 and 5 reveal that our Query2GMM demonstrates superior performance compared to the baselines in most cases. This is in alignment with the analysis provided in the main paper.

## B.3 Additional Ablation Study

We construct more ablation studies on intersection operation to show the effectiveness of the proposed co-attention network as shown in Table 6. We create two variants, i.e., Query2GMM<sub>inter2</sub> and Query2GMM<sub>inter3</sub>. Concretely, we replace the co-attention network with cross-attention followed by self-attention (Query2GMM<sub>inter2</sub>), which results in a performance decline of up to 3.7%. This implies that solely leveraging query-level exploration with fine-tuning techniques is not adequate for fitting the  $m$ -intersected answer area. For the variant Query2GMM<sub>inter3</sub>, we remove the cross-attention network from our co-attention network. This leads to a performance drop of up to 5.7%, indicating the necessity of learning inter-query level correlations for the intersection operator.

Besides, we observe that Query2GMM<sub>inter3</sub> outperforms Query2GMM<sub>inter</sub> (in Table 2 in main paper) across all query structures with the intersection. This suggests that attention-pooling can assist in adaptively generating more precise answer areas based on the output of global self-attention, as compared to the random sampling used in Query2Particles [6].

Table 4: Hit@3 results (%) for answering EPFO queries on FB15k, FB237, and NELL. The best result is highlighted in bold.

Dataset	Method	Query									
		1p	2p	3p	2i	3i	ip	pi	2u	up	AVG
FB15k	BetaE	73.3	27.1	26.5	62.1	73.3	29.8	48.7	45.2	26.6	45.8
	PERM	77.2	35.4	31.5	63.0	74.2	26.7	44.2	57.9	25.4	48.4
	NMP-QEM	80.9	40.8	34.9	61.3	71.8	25.5	46.3	62.0	28.2	50.2
	Q2P	84.5	49.9	43.3	70.0	78.3	24.7	48.2	71.7	30.5	55.7
	LMPNN	89.1	46.4	34.3	<b>73.1</b>	81.8	<b>52.9</b>	<b>48.4</b>	38.0	<b>37.7</b>	55.7
	Ours	<b>91.2</b>	<b>58.1</b>	<b>48.7</b>	72.7	<b>82.0</b>	29.5	47.1	<b>75.1</b>	31.3	<b>59.5</b>
FB237	BetaE	43.0	10.7	10.0	32.7	47.6	12.5	24.5	12.5	9.9	22.6
	PERM	46.8	24.2	19.8	30.8	42.4	12.2	22.1	20.8	11.7	25.6
	NMP-QEM	48.3	19.2	15.0	35.2	47.1	11.5	24.4	19.2	13.8	26.0
	Q2P	40.3	26.9	23.4	32.3	47.9	11.5	22.1	21.0	18.2	27.1
	LMPNN	49.7	13.8	11.0	<b>40.4</b>	<b>55.7</b>	<b>24.9</b>	18.4	13.4	11.0	23.6
	Ours	<b>51.7</b>	<b>31.0</b>	<b>24.7</b>	39.7	55.0	11.5	<b>25.7</b>	<b>26.8</b>	<b>19.4</b>	<b>31.7</b>
NELL	BetaE	58.9	14.0	11.9	42.2	53.8	16.6	26.9	13.3	9.4	27.4
	PERM	49.9	22.2	19.6	33.5	48.2	13.0	18.5	32.0	19.5	28.5
	NMP-QEM	56.8	25.3	21.4	36.5	48.8	16.2	22.0	25.2	15.6	29.8
	Q2P	60.0	31.4	31.7	32.5	49.9	11.6	19.7	42.3	21.4	33.4
	LMPNN	63.8	23.2	18.4	<b>44.6</b>	56.4	<b>29.2</b>	25.0	17.3	16.1	32.7
	Ours	<b>68.9</b>	<b>39.1</b>	<b>36.1</b>	44.3	<b>59.4</b>	17.0	<b>28.0</b>	<b>52.1</b>	<b>23.7</b>	<b>41.0</b>

Table 5: Hit@10 results (%) for answering queries with negation on FB15K, FB237, and NELL. The best result is highlighted in bold.

Dataset	Method	Query					AVG
		2in	3in	inp	pin	pni	
FB15k	BetaE	29.8	31.1	23.3	13.9	25.8	24.8
	NMP-QEM	35.5	35.4	22.9	16.0	31.8	28.3
	Q2P	41.3	40.2	24.2	18.8	33.6	31.6
	LMPNN	43.4	<b>46.1</b>	<b>30.2</b>	<b>23.3</b>	29.6	<b>34.5</b>
	Ours	<b>43.8</b>	45.1	26.5	20.2	<b>34.3</b>	34.0
FB237	BetaE	10.4	17.0	15.8	7.5	6.7	11.5
	NMP-QEM	12.0	18.4	15.5	9.1	7.2	12.4
	Q2P	10.1	20.7	16.7	9.9	7.2	12.9
	LMPNN	14.9	25.7	17.1	10.2	<b>9.0</b>	15.4
	Ours	<b>16.3</b>	<b>28.6</b>	<b>18.8</b>	<b>12.7</b>	8.7	<b>17.0</b>
NELL	BetaE	11.5	17.8	20.8	6.6	6.6	12.7
	NMP-QEM	11.9	19.7	17.4	8.7	7.0	12.9
	Q2P	12.1	18.2	21.4	7.0	7.6	13.3
	LMPNN	16.2	22.9	24.4	8.3	10.2	16.4
	Ours	<b>19.5</b>	<b>27.2</b>	<b>27.4</b>	<b>11.1</b>	<b>11.1</b>	<b>19.3</b>

#### B.4 Training Time Comparison

To evaluate the efficiency of the proposed Query2GMM, we perform experiments on the NELL dataset and report the offline training time. We can observe from Fig. 5 that Query2GMM takes a slightly longer training time than LMPNN (excluding pre-training time), achieving the second-best performance in efficiency. Probabilistic distribution-based methods (i.e., BetaE, PERM, NMP-QEM) require longer training time than our Query2GMM. This demonstrates the efficiency of our proposed



Table 6: MRR results (%) for ablation study on intersection operation on NELL dataset. The best result is highlighted in bold.

Method	Query			
	2i	3i	ip	pi
Query2GMM	<b>39.8</b>	<b>54.7</b>	<b>16.1</b>	<b>25.7</b>
Query2GMM <sub>inter2</sub>	36.6	52.5	14.6	22.0
Query2GMM <sub>inter3</sub>	34.4	50.9	14.6	20.0
Query2GMM <sub>inter</sub>	32.6	42.5	14.2	19.4

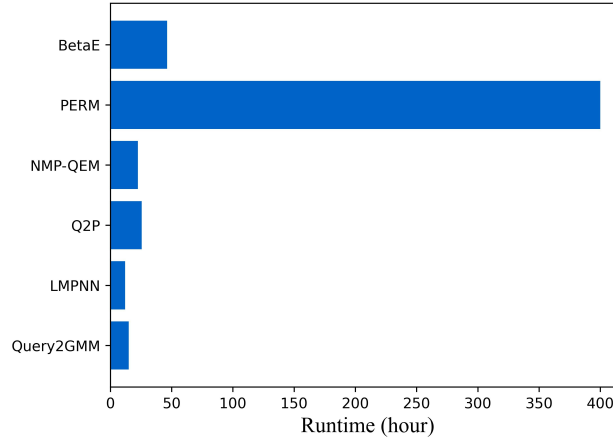


Figure 5: Training Time of different methods on NELL dataset.

embedding backbone (i.e., GMM embedding), which is based on univariate Gaussian distribution coupled with the Cartesian product.